Nuclear Physics **A518** (1990) 561-571
North-Holland

BACKWARD ANGLE np DIFFERENTIAL CROSS SECTIONS FROM 22 TO 50 MeV

G. FINK, P. DOLL, T.D. FORD[1], R. GARRETT[2], W. HEERINGA, K. HOFMANN[3], H.O. KLAGES and H. KRUPP[4]

Kernforschungszentrum Karlsruhe, Institut für Kernphysik I, Postfach 3640, D-7500 Karlsruhe, Fed. Rep. Germany

Received 17 April 1990
(Revised 21 June 1990)

Abstract: High-precision measurements of the backward angular shape of the differential cross section for neutron-proton scattering are reported. The new results considerably improve the np data base in the energy range from 22 to 50 MeV. Phase-shift analyses including all available np scattering data show reduced uncertainties, especially in the $^1P_1$ ($T=0$) phase shift.

E NUCLEAR REACTIONS ^{1}H(n, n), $E=22$-50 MeV; measured σ (E, Θ). Polyethylene target.

1. Introduction

At the Karlsruhe cyclotron a program is underway to measure np scattering observables with polarized and unpolarized particles, using the polarized neutron facility POLKA [1]). The data base for the np system is still rather small and is of limited accuracy. On the other hand, the number of phase shifts required to describe np scattering is twice that for pp scattering, because both isospin singlet ($T=0$) and isospin triplet ($T=1$) phase shifts contribute. Therefore there is a need for more, and for more accurate, np data. Large and accurate np and pp data bases would allow comparison of independently determined $T=1$ phase shifts from both systems.

Small differences in np and pp phase shifts can be expected from charge independence breaking (CIB), e.g. due to quark mass differences. Theoretical calculations of such anomalous (due to the strong interaction) isospin violating effects are still very premature. Langacker and Sparrow [2]) considered the effects of an isospin-violating potential with $\pi\eta$ and $\rho\omega$ mixing. Henley and Zhang [3]) calculated the effects of quark mass differences on the meson-nucleon coupling constants.

[1] Present address: FIZ, Karlsruhe, Fed. Rep. Germany.
[2] Permanent address: University of Auckland, New Zealand.
[3] Present address: SEL, Pforzheim, Fed. Rep. Germany.
[4] Present address: Siemens AG, München, Fed. Rep. Germany.

The Nijmegen group has recently carried out a phase-shift analysis of np scattering data below 25 MeV [ref. [4])]. The NN interaction used by them leads to a parametrization of the $^3P_1$ and $^1D_2$ phase shifts in terms of Δg^2, the difference between the charged and uncharged pion–nucleon coupling constants $g_c^2 = g^2(NN\pi^{\pm})$ and $G_0^2 = g^2(NN\pi^0)$. They find a large splitting, $\Delta g^2/g_0^2 \simeq (10 \pm 1)\%$, consistent with a value previously found by the same group from pp scattering up to 350 MeV [ref. [5])]. The np and pp data bases are too poor, however, to yield independently determined $T = 1$ phase shifts that can be compared with the phase-shift splittings predicted from this coupling constant splitting.

The various nucleon–nucleon observables show a different sensitivity to the phase shifts. Sensitivity calculations, such as carried out by Binstock and Bryan [6]), show that the S-waves mainly determine σ_{tot}; that the $^1P_1$ wave mostly affects the shape of $d\sigma/d\Omega$ and the spin correlation coefficients; that the ^3P waves mainly determine the magnitude of A_y; that the ^3D waves determine the shape of A_y; and that the influence of the mixing parameter ε_1 is most striking in the spin correlation coefficients.

Our research program comprises measurements of the shape of $d\sigma/d\Omega$, of A_y and of A_{yy} in order to pin down more accurately the P and ^3D wave phase shifts and ε_1. Existing correlations between $^1P_1$ and ε_1 may be overcome by first fixing $^1P_1$ by measurements of the angular shape of $d\sigma/d\Omega$ and subsequently determining ε_1 by A_{yy} measurements.

In this paper we report on high-accuracy measurements of the np differential cross section in the angular range from 75° to 165° (c.m.) for neutron energies between 22 and 50 MeV. Results of a new phase-shift analysis, taking into account all existing np data in this energy region, are presented.

The theoretical models with the most practical value in the last decade probably have been the one-boson exchange calculations from Bonn [7]) (Bonn-old), the semi-phenomenological Paris potential [8]), and the more recent Bonn calculations including multi-meson exchange [9]) (Bonn-new). Our data are compared with results from both latter models.

2. Experiment

The experiment was carried out using the neutron facility POLKA at the Karlsruhe cyclotron. It provides a polarized neutron beam with a continuous energy distribution between 20 and 50 MeV. The beam is pulsed with a repetition rate of 11 MHz. Time-of-flight (t.o.f.) methods are used to determine the individual neutron energy. In the off-line analysis, neutron energy bins are defined by appropriate cuts in the t.o.f. spectrum. The neutron flux is monitored by a set-up of recoil proton telescopes. More details can be found elsewhere [1]).

The np scattering experiment was carried out at a distance of 6 m from the neutron source inside an evacuated scattering chamber of 80 cm diameter. The collimated

neutron beam (20 mm diameter) entered and left the scattering chamber through 25 μm thick stainless steel windows. The scattering target, a 30 mg/cm^2 polyethylene foil was positioned at the center. Neutron–proton scattering events were detected by measuring the recoil protons in ΔE-E telescopes. The ΔE detectors were 12×42 mm^2, 500 μm thick, passivated ion implanted silicon detectors. The proton energy was measured with 2.5 cm thick NaI crystals. A number of 5 telescopes were available, which were used to measure the protons at lab angles from 7.5° to 52.5°. They were mounted on rotatable rings inside the scattering chamber. To reduce systematic errors, each scattering angle was measured, both left and right, by at least three different ΔE-E telescopes in the course of the experiment. The properties of the telescopes are described in detail in ref. [10]).

Computer simulations of the kinematics of the experiment have been carried out to recognize the angular and energy regions, which can contain background from (n, p) reactions on the carbon contained in the polyethylene target. Following these simulations the target thickness and detector dimensions were optimized accordingly. The amount of background was determined in a separate experiment by scattering from a carbon target of appropriate thickness.

Each event was characterized by the pulse heights in the ΔE and E detectors, the total time-of-flight between the neutron source and the ΔE-E telescope, and the telescope number. All parameters were written on magnetic tape using an ND4420 data acquisition system. On-line monitoring of one- and two-dimensional spectra was carried out during the experiment. Data were taken for about 300 h, divided into runs of about 2 h length.

3. Data analysis

The parameters of the event matrix are subject to variations during the experiment. The t.o.f. spectra may shift due to phase instabilities of the cyclotron, and the ΔE and E pulse-height spectra may vary due to gain changes in the electronics. The first step of the data analysis was to correct for these effects.

In the course of the experiment the ΔE-E telescopes were operated at various angles, each with a characteristic proton recoil energy spectrum due to kinematics. This provided the possibility of correction for small nonlinearities present in some detectors, as well as differences in resolution. These were accounted for in the subsequent data handling.

The next step was to remove background by applying cuts in the two-dimensional projections of the event matrix. Fig. 1 shows an example of a ΔE versus E matrix, in which the data of several telescopes have been added. It exhibits an excellent separation of the light charged reaction products, thus enabling discrimination against other particles than protons.

A small portion of the protons, up to 2% depending on proton energy, do not deposit their full energy inside the NaI detector. Part of their energy is missing due

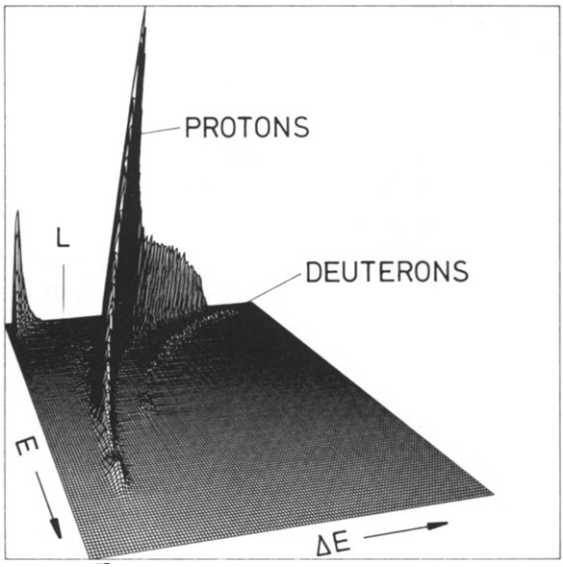

Fig. 1. ΔE versus E event matrix recorded with several telescope systems at scattering angles between 7.5° and 52.5° (lab.). The region L is discussed in the text.

to: (1) reactions with a negative Q-value; (2) production of neutrons or gamma rays which escape from the detector; (3) production of heavier charged particles for which the detector response is not linear. For mono-energetic protons this leads to a rather flat distribution almost down to zero energy. In fig. 1 these events can be found in the region indicated by L (loss) between the proton ridge and the $E=0$ axis. They are not visible in the figure, because few events are smeared out rather evenly. We have integrated the counts found in this region and compared them to calculated values, based on known cross sections. These values agree well; hence other background in the L-region appears to be negligible.

Background due to (n, p) reactions on carbon was separated out in t.o.f. versus E-matrices. For this purpose the simulations of the reaction kinematics turned out to be very useful. Fig. 2 shows a t.o.f. versus E matrix, measured at a proton detection angle of 7.5° (lab). This matrix still contains the events from the 'L' region as discussed above. It shows a very good separation between protons from np scattering and from (n, p) reactions on ^{12}C. The strong angular dependence of the np scattering kinematics inhibits this separation for laboratory angles greater than 30°. For these angles background was subtracted, using data obtained with a pure carbon target in a separate experiment. At smaller angles, this carbon background is negligible when the appropriate cuts have been applied to the data.

The effective scattering angles and the angular resolutions were calculated by a Monte Carlo simulation, but these corrections had very little influence on the results.

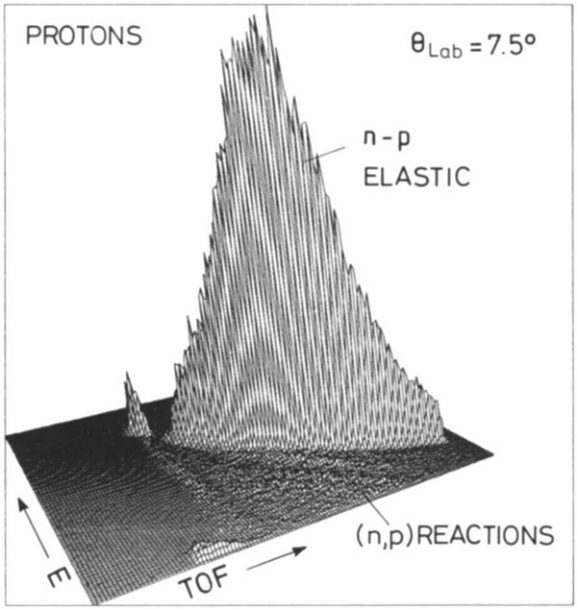

Fig. 2. Time-of-flight versus E event matrix at 7.5° (lab).

The different detectors exhibited slightly different solid angles, which were corrected for.

Finally the np scattering count rates, normalized to the incident neutron flux, were determined in eight energy bins and for six neutron scattering angles from 90° to 165° c.m. For the lowest neutron energy bins, not all angles could be analyzed due to threshold effects from the energy loss of the protons in the target and in the ΔE detector.

Uncertainties in the data correction procedure and systematic differences in detector properties were taken into account, resulting in the determination of systematic errors [11]). The total errors given are dominated by the statistical uncertainties.

In fig. 3 our new data are shown, given in absolute values for $d\sigma/d\Omega$. The experiment itself only yields relative values for the differential cross sections. The procedure used to normalize our relative data by means of phase-shift analyses is described in the next section. The numerical values are listed in table 1.

4. Phase-shift analyses

The normalization of the cross-section data was attained using phase-shift analyses. The first approximation was obtained by setting the 120° data point at each energy bin to the value predicted by the Paris potential [8]). Subsequently, these distributions were used as additional input in phase-shift analyses using all available

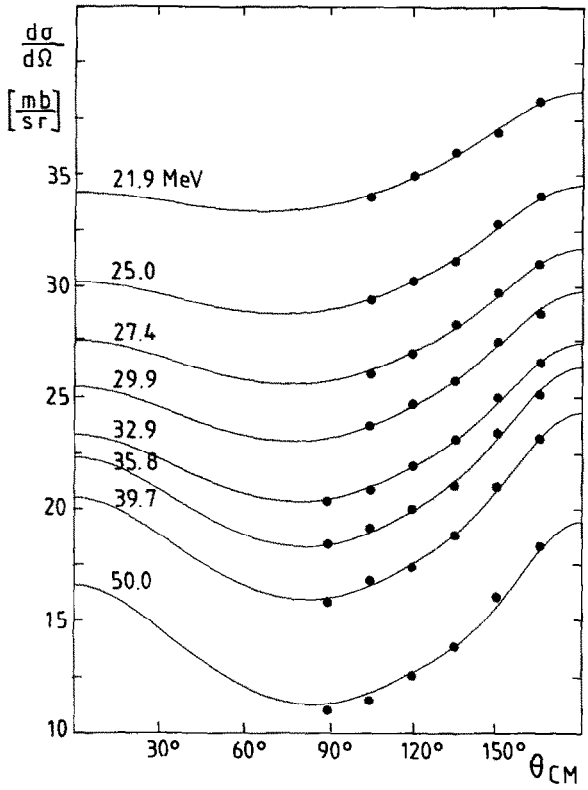

Fig. 3. Measured np differential cross sections of this experiment. The curves are the results of our phase-shift analyses.

np scattering data in the energy range 15–50 MeV. A detailed list of references can be found in ref. [11]). In the χ^2 search, the normalizations of the new data sets were allowed to be totally free. Because of the small data base, no true single-energy analysis was possible for each energy bin. Instead, an analysis using five partly overlapping energy regions between 16 and 50 MeV was carried out [11]). The starting values for the phase shifts and their energy dependence were taken from the Paris potential. The higher ($J \geqslant 4$) partial waves were kept fixed. In the beginning, both the $T=0$ and the $T=1$ phase shifts were determined from np data exclusively.

In the first calculations, only previously existing data were analyzed. Different starting conditions and restrictions in phase shifts and normalization parameters were studied. The normalization parameters for all data sets remained stable within their errors and could be fixed further on. This considerably reduced the number of free parameters in the subsequent analysis.

After this procedure our data were included with free normalization; thus only the shape of $d\sigma/d\Omega$ had an influence in the phase-shift analysis. We started with no constraints on the phase shifts. The phases $^1P_1$, $^3D_3$ and ε_1 remained free during

TABLE 1

np differential cross sections [mb/sr]

$\Theta_{c.m.}$	E-BIN: $\bar{E}$ =	22.0±1.5 MeV 22.2 MeV	25.0±1.5 MeV 25.0 MeV	27.5±1.5 MeV 27.4 MeV	30.0±1.5 MeV 29.9 MeV
104.6°		34.00±0.19	29.39±0.16	26.26±0.18	23.80±0.16
119.6°		34.93±0.17	30.22±0.14	27.17±0.15	24.76±0.14
134.7°		35.97±0.18	31.17±0.15	28.50±0.17	25.77±0.15
149.8°		36.92±0.19	32.78±0.16	29.96±0.18	27.52±0.16
164.9°		38.27±0.17	34.02±0.15	31.22±0.16	28.80±0.15
$\Theta_{c.m.}$	E-BIN: $\bar{E}$ =	33.0±1.5 MeV 32.9 MeV	36.0±1.5 MeV 35.8 MeV	40.0±2.0 MeV 39.7 MeV	50.0±2.0 MeV 50.0 MeV
89.4°		20.39±0.19	18.49±0.21	15.89±0.23	11.02±0.21
104.4°		20.90±0.18	19.17±0.20	16.85±0.22	11.47±0.21
119.5°		21.95±0.15	20.05±0.18	17.44±0.19	12.58±0.19
134.6°		23.14±0.16	21.16±0.19	18.89±0.20	13.88±0.20
149.7°		25.03±0.18	23.48±0.21	21.09±0.23	16.10±0.23
164.8°		26.58±0.16	25.16±0.19	23.21±0.20	18.36±0.22

the whole procedure. It appeared that the results for the $^3P_2$, $^3D_1$ and $^3D_2$ phase shifts were in good agreement with the predictions of the Paris potential. These phase shifts were then fixed to the predictions of the Paris potential. The $^1S_0$, $^3S_1$ and $^3P_0$ phase shifts also agreed well with those given by the Paris potential in the energy region between 20 and 30 MeV, and in this region they were fixed to the Paris potential values. Correlations between some phase shifts, especially those for the ^3P waves, made it necessary to take the $^3P_1$ and the $^1D_2$ phase shifts from the pp system [12]).

In this way we obtained normalization factors for our differential cross sections which turned out to be stable within ±1% for any reasonable change in data base or in parameter constraints in various independent phase-shift searches. We take this variation as a measure for the uncertainty in our final scaling factors and interpret it as the systematic error of the absolute values of $d\sigma/d\Omega$ derived in this way. This scale error is not included in the uncertainties for each data point listed in table 1.

5. Results and discussion

The present experiment and subsequent phase-shift analysis has yielded a large amount of high-accuracy np cross section data between 22 and 50 MeV with errors of the order of (1–2)%.

In figs. 4 and 5 they are compared with older measurements, which only exist in the energy region around 25 MeV [refs. [13–17])] and around 50 MeV [refs. [16,18])].

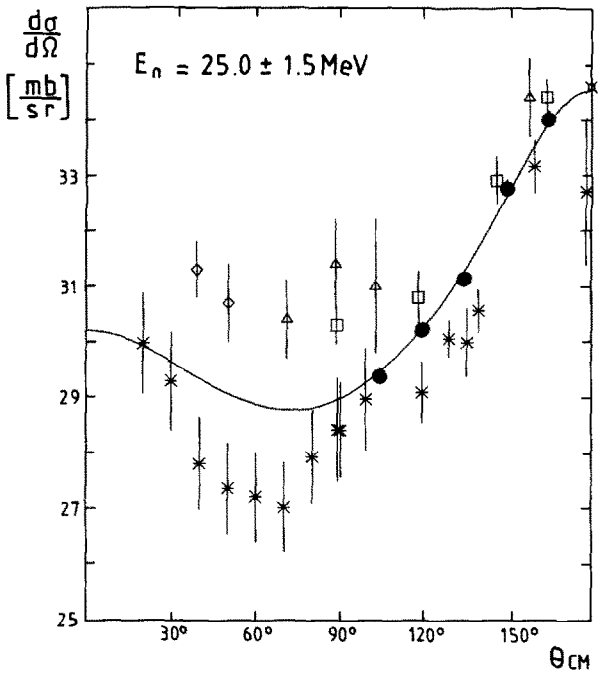

Fig. 4. Comparison of our data (dots) at 25 MeV with other data at nearby energies. Squares: ref. [13]) (24.0 MeV); triangles: ref. [14]) (24.0 MeV); diamonds: ref. [15]) (24.0 MeV); stars: ref. [16]) (25.8 MeV); stardot: ref. [17]) (25.3 MeV). The curve is the result of our phase-shift analysis.

Around 25 MeV (fig. 4), our data have uncertainties a factor of 3 to 6 smaller than those of the previous data, which are at slightly different energies. The Madison data at 24.0 MeV are partly relative cross sections measured with counter telescopes, which were normalized to total cross section calculations [13,14]) and partly consist of absolute cross sections, for which the intensity of the scattered neutrons and of the 0° incident neutron beam were both measured [15]). The Davis data at 25.8 MeV are relative cross sections normalized to σ_{tot} [ref. [16])]. The shape of our angular distribution agrees well with those of the older data. The absolute values are also in agreement, although the values at 24 MeV are higher and those at 25.8 MeV lower than ours at 25 MeV, as is expected from the energy dependence of the total cross section.

The agreement of our data with the absolute 180° cross sections measured at Los Alamos [17]) at 25.3 and 31.1 MeV is excellent. These absolute cross sections were obtained by comparing the proton yields in a counter telescope with the neutron flux measured with a calibrated time-of-flight system and by subsequent normalization to the value of 62.9 mb/sr for neutrons of 12.83 MeV. This agreement supports the reliability of the procedure of normalizing our data by a phase shift analysis.

The POLKA results agree very well with those of the Davis group [16]) at 50 MeV (fig. 5), which are also relative measurements but normalized to σ_{tot}. Our data

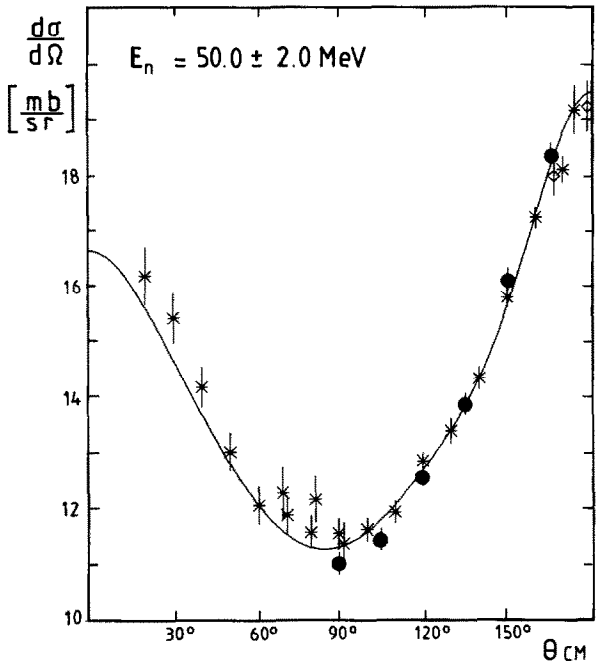

Fig. 5. Comparison of our data (dots) at 50 MeV with other data at this energy. Stars: ref. [16]); diamonds: ref. [18]). The curve is the result of our phase-shift analysis.

exhibit errors of the same size, or at backward angles nearly a factor of two less. We confirm the backward-angle shape, which is different from the predictions of the Paris potential, as discussed below. There is also good agreement with 178.5°/90° and 166°/90° cross section ratios measured at Louvain-la-Neuve [18]). The older data of the same group [19]) have been withdrawn by the authors.

The phase-shift analysis yielding the normalization factors of our data resulted in a solution in which nearly all phase shifts are in agreement, within their errors, with those of the Paris potential. The χ^2-values per data point are close to 1.0 in all 5 energy bins ($\chi^2/P = 0.93$ for all 44 data points).

The results for the $^1P_1$ phase shift are shown in fig. 6. There is a remarkable improvement compared to older experimental phase-shift results. Our new results seem to lie somewhat above the predictions from the Bonn and Paris potentials. This shift toward less negative $^1P_1$ values implies a less steep angular distribution in the backward region.

It is apparent that the cross section shape, e.g. expressed in the form of the ratio $d\sigma(170°)/d\sigma(90°)$ is a good measure and test for potential predictions. In fig. 7 we compare the ratios derived from our phase-shift analyses at five energies with other experimental ratios [16,18,20,21]), partly derived by interpolation, and with those predicted by the Paris potential. All experimental ratios appear to be slightly below the Paris prediction.

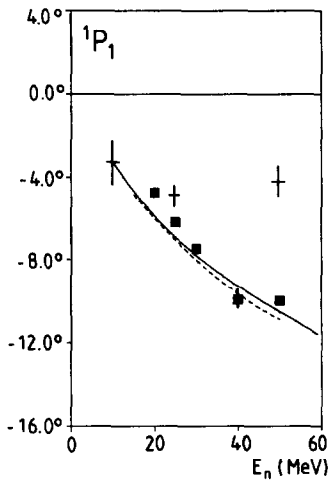

Fig. 6. Our results (filled squares) for the $^1P_1$ phase shift compared to results of a phase-shift analysis from ref. [12]) (crosses) and theoretical predictions from ref. [7]) (solid line) and ref. [8]) (dashed line).

6. Summary and outlook

A high-precision measurement of the np differential cross section was carried out with a continuous energy neutron beam. In general the new data have much smaller uncertainties than those of previous results. The new measurements of $d\sigma/d\Omega$ improve decisively the data base of the np system.

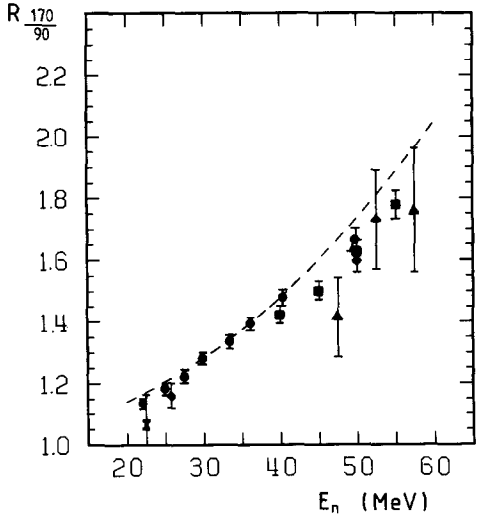

Fig. 7. Our experimental results (filled dots) for the ratio of the 170° to 90° np elastic cross section compared with results from ref. [16]) (diamonds), ref. [18]) (squares) and ref. [20]) (triangles). The single data point at 22.5 MeV stems from ref. [21]). The curve is a calculation from the Paris potential [8]).

Phase-shift analyses indicate much reduced uncertainties in the $^1P_1$ phase shift. A re-measurement of A_y data with higher precision is necessary to put better constraints on the ^3P and the $^3D_3$ phase shifts. There is a need for much more precise A_{yy}-data, because the knowledge about ε_1 is still very insufficient.

It will not be possible to evaluate both the $T=0$ and the $T=1$ phase shifts from np data before there is a rich, high precision data base. Then one could try to compare the $T=1$ phase shifts from the pp and np systems to check anomalous isospin violation in nucleon-nucleon forces due to quark mass differences.

The authors would like to thank Drs. V. Bechthold, L. Friedrich and H. Schweickert for providing the polarized deuteron beam. The help of V. Eberhard, P. Jany, Chr. Wölfl, W. Nitz, D. Reppenhagen, G. Schmalz, H. Skacel and G. Völker during the data-taking is gratefully acknowledged.

References

1) H.O. Klages, H. Dobiasch, P. Doll, H. Krupp, M. Oexner, P. Plischke, B. Zeitnitz, F.P. Brady and J.C. Hiebert, Nucl. Instr. Meth. **219** (1984) 269
2) P. Langacker and D.A. Sparrow, Phys. Rev. **C25** (1982) 1194
3) E.M. Henley and Z.-Y. Zhang, Nucl. Phys. **A472** (1987) 759
4) V.G.J. Stoks *et al.*, Phys. Rev. Lett. **61** (1988) 1702
5) J.R. Bergervoet *et al.*, Phys. Rev. Lett. **59** (1987) 2255
6) J. Binstock and R. Bryan, Phys. Rev. **D9** (1974) 2528
7) R. Machleidt, private communication, 1982;
K. Holinde and R. Machleidt, Nucl. Phys. **A247** (1975) 495;
K. Holinde, Phys. Reports **68** (1981) 121
8) B. Loiseau, private communication, 1984;
M. Lacombe, B. Loiseau, J.M. Richard, R. Vinh Mau, J. Cote, B. Pires and R. de Tourreil, Phys. Rev. **C21** (1980) 861;
W.N. Cottingham, M. Lacombe, B. Loiseau, J.M. Richard and R. Vinh Mau, Phys. Rev. **D8** (1973) 800
9) R. Machleidt, K. Holinde and Ch. Elster, Phys. Reports **149** (1987) 1
10) P. Doll, G. Fink, F.P. Brady, R. Garrett, H.O. Klages and H. Krupp, Nucl. Instr. Meth. **250** (1986) 526
11) G. Fink, diploma thesis, Univ. Karlsruhe (1986), unpublished
12) The calculations were made using Scattering Analysis Interactive Dial-Up (SAID), Virginia Polytechnic Institute, Blackburg VA, USA (R.A. Arndt, private communication).
13) L.N. Rothenberg, Phys. Rev. **C1** (1970) 1226
14) T.W. Burrows, Phys. Rev. **C7** (1973) 1306
15) T.G. Masterson, Phys. Rev. **C6** (1972) 690
16) T.C. Montgomery, B.E. Bonner, F.P. Brady, W.B. Broste and M.C. McNaughton, Phys. Rev. **C16** (1977) 499
17) M. Drosg and D.M. Drake, Nucl. Instr. Meth. **160** (1979) 143
18) A. Bol, C. Dupont, P. Leleux, P. Lipnik, P. Macq and A. Ninane, Phys. Rev. **C32** (1985) 308
19) A. Bol, C. Dupont, P. Leleux, P. Lipnik, P. Macq and A. Ninane, Proc. Few Body X, Karlsruhe 1983, ed. B. Zeitnitz, vol. II (North-Holland, Amsterdam, 1984) p. 23
20) J.P. Scanlon, G.H. Stafford, J.J. Thresher, P.J. Bowen and A. Langsford, Nucl. Phys. **41** (1963) 401
21) E.R. Flynn and P.F. Bendt, Phys. Rev. **128** (1962) 1268